Combined Measurements of Higgs Boson Production and Decay in the $H \to ZZ^* \to 4l$ and $H \to \gamma\gamma$ Channels

Kunlin Ran
IHEP, CAS

CLHCP 2017
Nanjing University, Nanjing

Higgs productions and decays

Higgs production modes

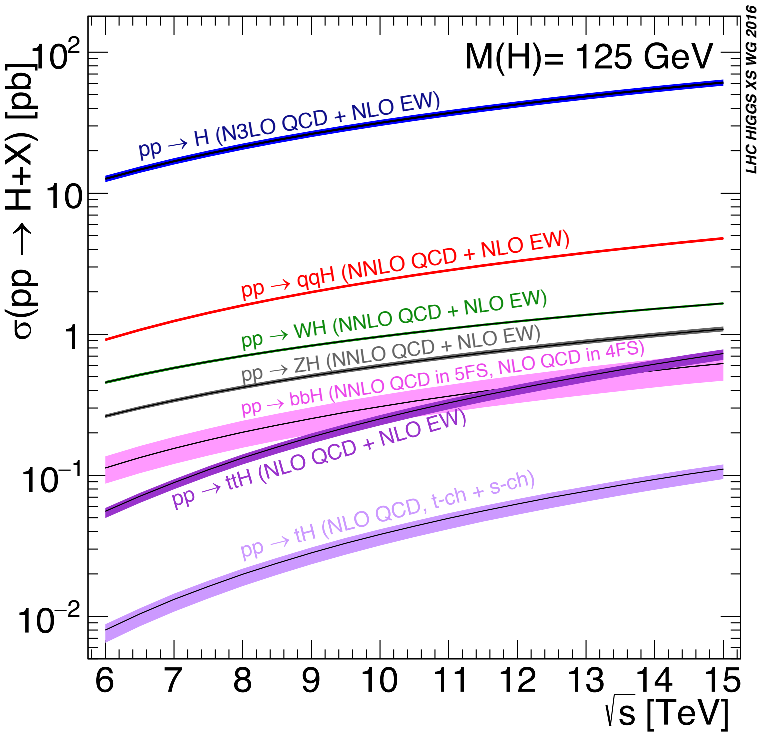

Higgs decay channels

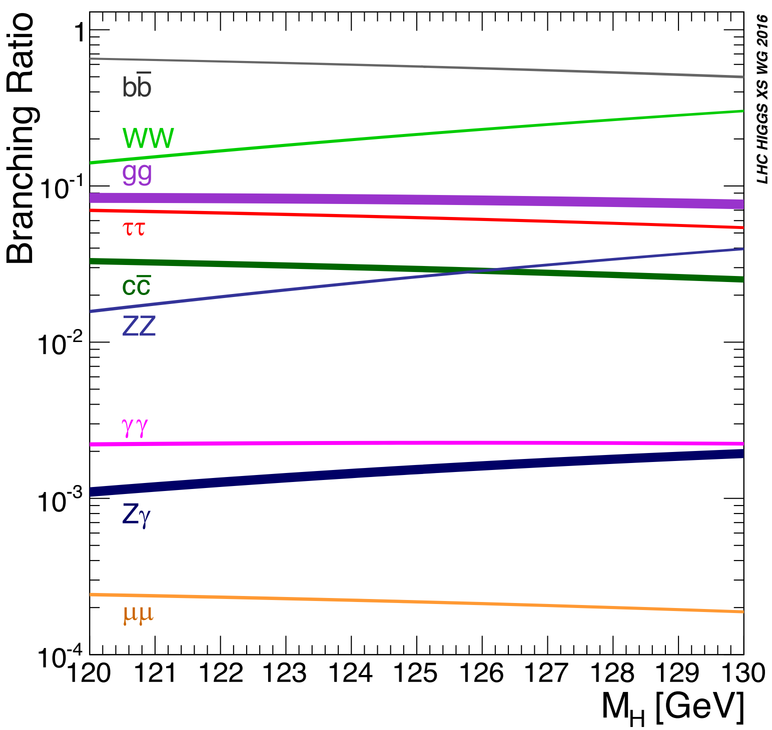

[CERN–2017–002-M]

- A broad range of measurements of Higgs properties have been performed using proton–proton collision data produced by LHC

Motivation and Introduction

- The combination of Higgs-boson decay channels could maximize the precision of these measurements

[Run I results]

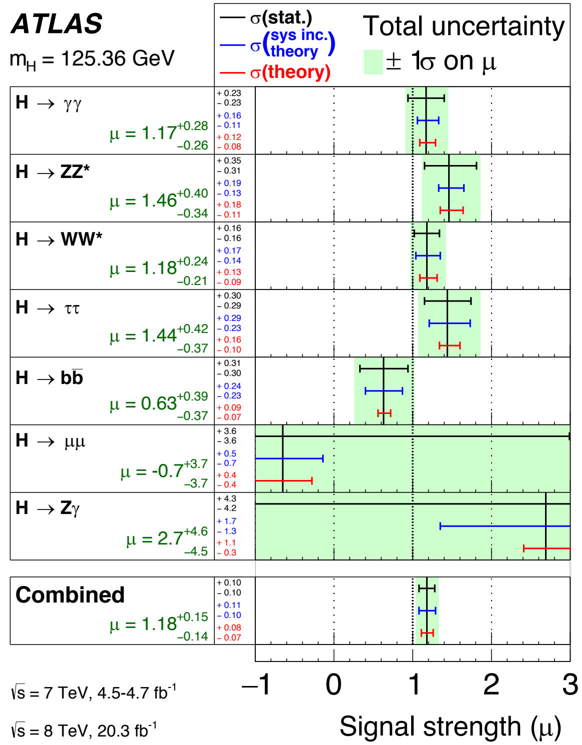

- In Run II, we presents the combination of measurements of Higgs boson production in the $H \rightarrow \gamma\gamma$ and $H \rightarrow ZZ^* \rightarrow 4l$ decay channels for now (ATLAS-CONF-2017-047)

Introduction

- We presents combination measurements
  - Total cross section
  - Global signal strength
  - Production cross sections/Ratio of cross sections
  - Simplified template cross sections
  - κ framework
    - κ_f, κ_V
    - κ_g, κ_γ
    - Generic model

- All measurements are performed assuming
  - $M_H = 125.09 \pm 0.21(stat.) \pm 0.11(syst.)\ GeV$
  - $BR_{\gamma\gamma} = (2.27 \pm 0.07)\times 10^{-3}$
  - $BR_{4l} = (1.251 \pm 0.027)\times 10^{-4}$

- Data were collected in 2015 and 2016, at a centre-of-mass energy of 13 TeV, corresponds to an integrated luminosity of 36.1 fb^{-1}

Event categories

- The analyses of the individual decay channels separate the measured events into exclusive kinematic and topological categories

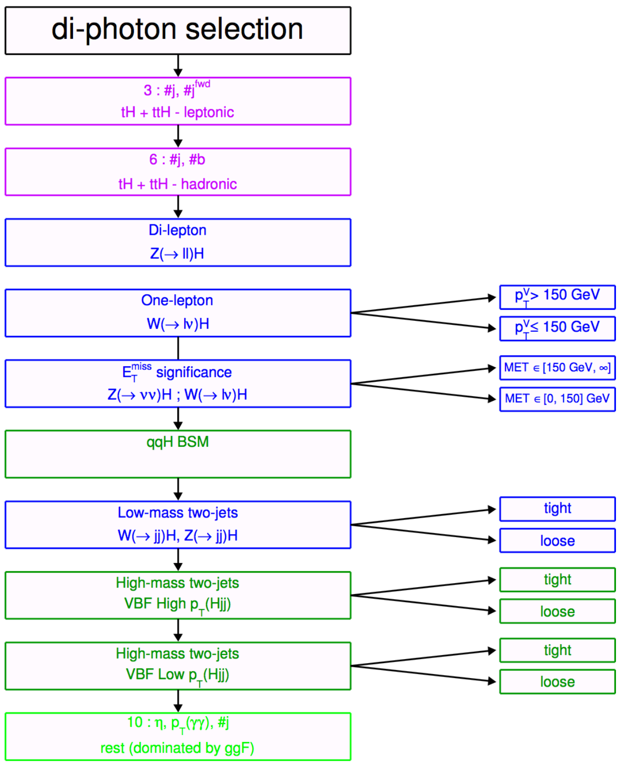

[ATL-COM-PHYS-2016-1784]

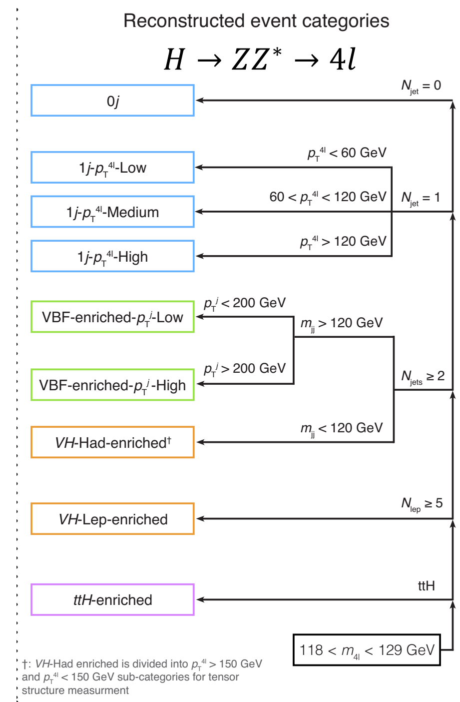

[CERN-EP-2017-206]

- The categories are structured hierarchically to prioritize the selection of signal events from processes with the smallest production cross sections
- A number of likelihood fits are presented to do combination measurements based on event categories

Global signal strength

- The global signal strength μ is defined as the ratio of the observed yield to its SM expectation
- $\mu = \frac{\sigma \times B}{(\sigma \times B)_{SM}}$

- $\mu_{\gamma\gamma} = 0.99 \pm 0.14 \left({}^{+0.12}_{-0.11}(stat.)^{+0.06}_{-0.05}(exp.)^{+0.06}_{-0.05}(th.)\right)$
- $\mu_{ZZ} = 1.28^{+0.21}_{-0.19} \left({}^{+0.18}_{-0.17}(stat.)^{+0.08}_{-0.06}(exp.)^{+0.08}_{-0.06}(th.)\right)$
- $\mu = 1.09 \pm 0.12 \left(\pm 0.09(stat.)^{+0.06}_{-0.05}(exp.)^{+0.06}_{-0.05}(th.)\right)$

- Run I result with all decay channels $(\gamma\gamma, ZZ^*, Z\gamma, WW^*, b\bar{b}, \tau\tau, \mu\mu)$
- $\mu = 1.18^{+0.15}_{-0.14} \left(\pm 0.10(stat.) \pm 0.07(exp.)^{+0.08}_{-0.07}(theo.)\right)$

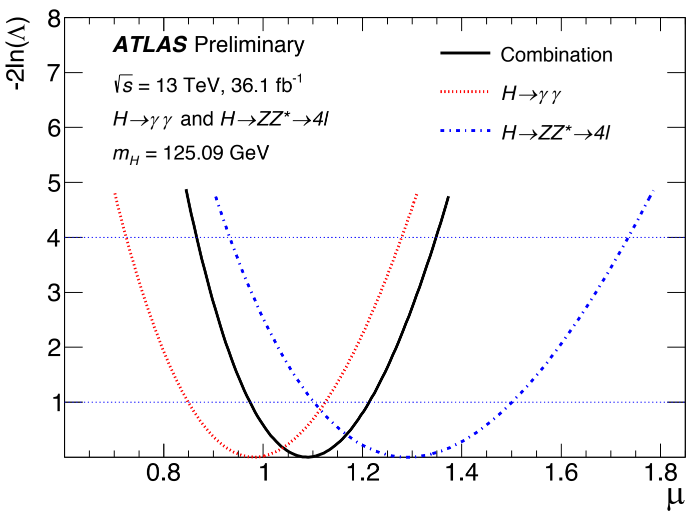

- Comparing to Run I results, errors decrease by 14%
- Comparing to individual decay measurements, errors decrease by 22%/30% ($\gamma\gamma/ZZ^*$)

- The measurement is consistent with the SM prediction with a p-value of $p_{SM} = 47\%$

- The leading uncertainties are
  - Theoretical: σ_{ggF}^{SM}, PDFs, Branching fractions and α_S
  - Experimental: Luminosity, Energy resolution (e, γ) and Pileup

Total cross section

- The total $pp \to H + X$ cross sections at centre-of-mass energies of 7, 8 and 13 TeV are measured in data corresponding to integrated luminosities of $4.5\ fb^{-1}$, $20.3\ fb^{-1}$and $36.1\ fb^{-1}$

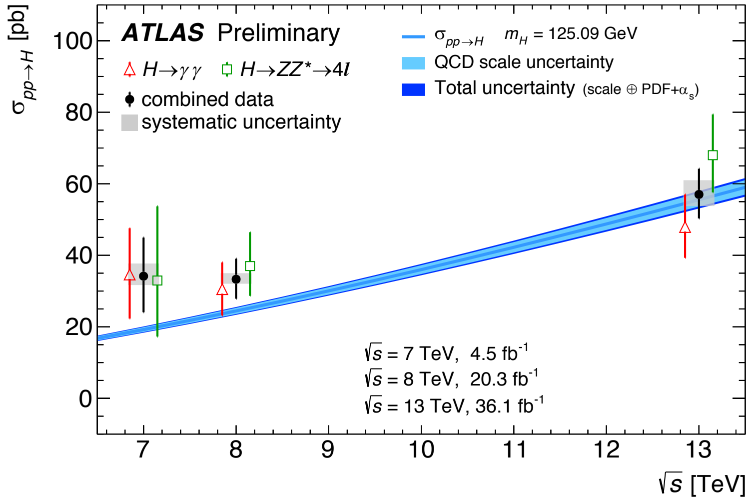

Decay channel	Total cross section ($pp \to H + X$)		
	$\sqrt{s}$ =7 TeV	$\sqrt{s}$ =8 TeV	$\sqrt{s}$ =13 TeV
$H \to \gamma\gamma$	35^{+13}_{-12} pb	$30.5^{+7.5}_{-7.4}$ pb	$47.9^{+9.1}_{-8.6}$ pb
$H \to ZZ^* \to 4\ell$	33^{+21}_{-16} pb	37^{+9}_{-8} pb	$68.0^{+11.4}_{-10.4}$ pb
Combination	34 ± 10 (stat.) $^{+4}_{-2}$ (syst.) pb	$33.3^{+5.5}_{-5.3}$ (stat.) $^{+1.7}_{-1.3}$ (syst.) pb	$57.0^{+6.0}_{-5.9}$ (stat.) $^{+4.0}_{-3.3}$ (syst.) pb
SM prediction [8]	19.2 ± 0.9 pb	24.5 ± 1.1 pb	$55.6^{+2.4}_{-3.4}$ pb

- The systematic uncertainties are smaller than the statistical uncertainties for the measurements at all three center-of-mass energies
- The results of the individual decay channels are compatible with a p-value of 29%, and no deviation from the SM predictions is observed $(p_{SM} = 84\%)$

Production cross sections

- A combined fit is performed for the cross sections of ggF, VBF, VH, and $t\bar{t}H$ for $|y_H| < 2.5$ and assuming SM branching fractions
- The measurements of ggF and $t\bar{t}H$ production include the $b\bar{b}H$ and tHX processes

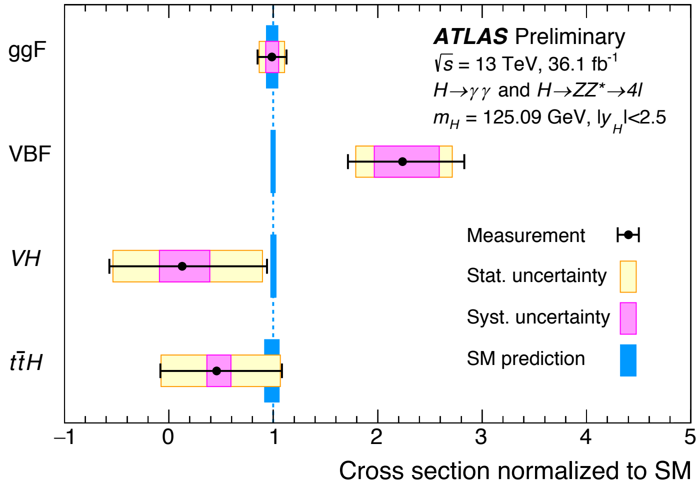

Process ($\|y_H\| < 2.5$)	Result [pb]	Uncertainty [pb] Total	Stat.	Exp.	Th.	SM prediction [pb]
ggF	43.9	$^{+6.2}_{-6.0}$	$^{+5.5}_{-5.4}$	$^{+2.7}_{-2.3}$	± 1.2	$44.5^{+2.0}_{-3.0}$
VBF	7.9	$^{+2.1}_{-1.8}$	$^{+1.7}_{-1.6}$	$^{+0.8}_{-0.6}$	$^{+1.0}_{-0.7}$	$3.52^{+0.08}_{-0.07}$
VH	0.3	$^{+1.6}_{-1.4}$	$^{+1.5}_{-1.3}$	± 0.4	$^{+0.3}_{-0.2}$	$1.99^{+0.06}_{-0.05}$
$t\bar{t}H$	0.27	$^{+0.37}_{-0.32}$	$^{+0.36}_{-0.31}$	$^{+0.06}_{-0.05}$	$^{+0.05}_{-0.02}$	$0.59^{+0.03}_{-0.05}$

- The four-dimensional compatibility between the measurement and the SM prediction corresponds to a p-value of $p_{SM} = 5\%$

VBF VS ggF

- The measurements of the ggF and VBF cross-sections are typically anti-correlated, since the selections used to identify VBF production also select some ggF production events
- The measured likelihood contours in the σ_{VBF} versus σ_{ggF} plane from $H \to \gamma\gamma$ and $H \to ZZ^* \to 4l$, and their combination

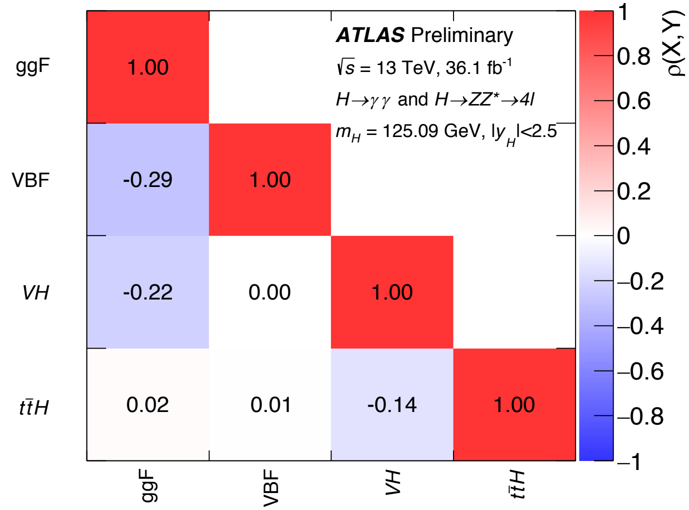

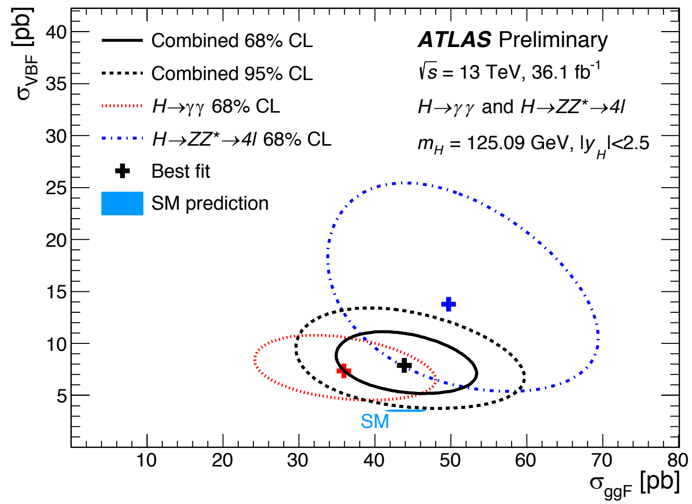

- The two-dimensional compatibility between the measurement and the SM prediction corresponds to a p-value of $p_{SM} = 3\%$

Ratios of cross sections and branching fractions

- To remove the assumption of the SM branching fractions of the Higgs boson
- A combined fit of the production cross-section ratios $\sigma_{VBF}/\sigma_{ggF}$, σ_{VH}/σ_{ggF}, and $\sigma_{t\bar{t}H}/\sigma_{ggF}$, the branching-fraction ratio $B_{\gamma\gamma}/B_{4l}$, and the product $\sigma_{ggF}\times B_{4l}$ divided by its SM prediction are presented
- Common systematic uncertainties cancel in these ratios, reducing model dependence and improving precision
- $\sigma_i \cdot B_f = \sigma_{ggF} \cdot B_{4l} \cdot \left(\frac{\sigma_i}{\sigma_{ggF}}\right) \cdot \left(\frac{B_f}{B_{4l}}\right)$

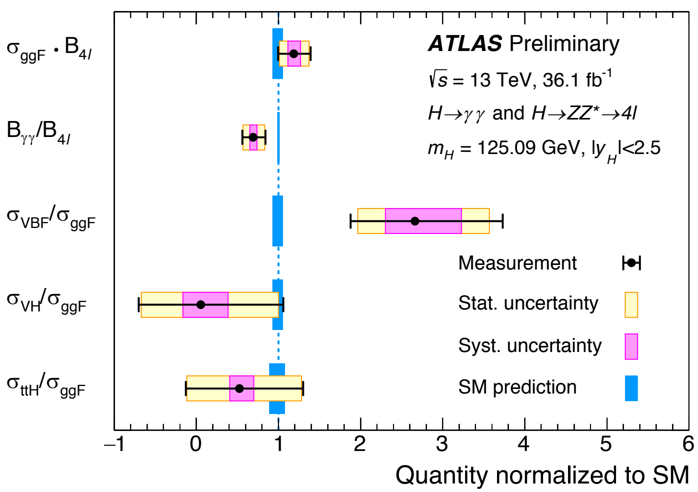

Quantity		Result	Uncertainty Total	Stat.	Exp.	Th.	SM prediction
$\sigma_{\rm ggF}\cdot B_{4\ell}$	[fb]	6.6	$^{+1.2}_{-1.0}$	$^{+1.1}_{-1.0}$	±0.4	±0.2	$5.6^{+0.3}_{-0.4}$
$B_{\gamma\gamma}/B_{4\ell}$		12.5	$^{+2.8}_{-2.3}$	$^{+2.6}_{-2.2}$	$^{+0.9}_{-0.7}$	±0.2	18.1 ± 0.2
$\sigma_{\rm VBF}/\sigma_{\rm ggF}$	$[10^{-2}]$	21.5	$^{+8.5}_{-6.3}$	$^{+7.3}_{-5.6}$	$^{+2.8}_{-1.7}$	$^{+3.6}_{-2.2}$	$7.9^{+0.4}_{-0.6}$
$\sigma_{VH}/\sigma_{\rm ggF}$	$[10^{-2}]$	0.2	$^{+4.5}_{-3.4}$	$^{+4.2}_{-3.2}$	$^{+1.2}_{-0.9}$	$^{+0.9}_{-0.4}$	$4.5^{+0.2}_{-0.3}$
$\sigma_{t\bar{t}H}/\sigma_{\rm ggF}$	$[10^{-2}]$	0.7	$^{+1.0}_{-0.9}$	$^{+1.0}_{-0.9}$	$^{+0.2}_{-0.1}$	±0.1	1.3 ± 0.1

- The five-dimensional compatibility between the measurements and the SM predictions corresponds to a p-value of $p_{SM} = 3\%$

Merged Stage1 STXS measurement

- The simplified template cross section framework defines a set of kinematic regions for each production process and combines these with the ratios of branching fractions for the various decay channels
- $y_j = \sum_i A_{ji} \cdot r_i \cdot (\sigma_i \cdot B_{4l})_{SM} \cdot r_f \cdot \left(\frac{B_f}{B_{4l}}\right)_{SM} \cdot \mathcal{L}$
- By dividing the cross sections into kinematic regions, the framework reduces the reliance on the SM for cross-section measurements

- The current data sets are not sensitive to the SM production of the full set of stage-1 processes
- Lower-rate regions are merged in order to give sensitivity to SM production and to minimize correlations

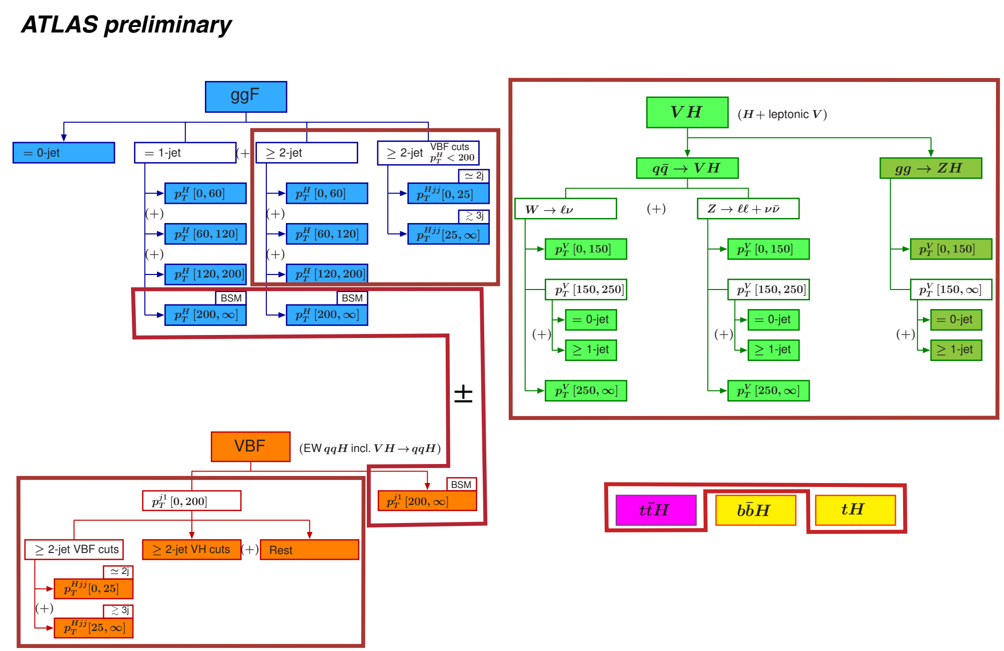

Simplified template cross sections

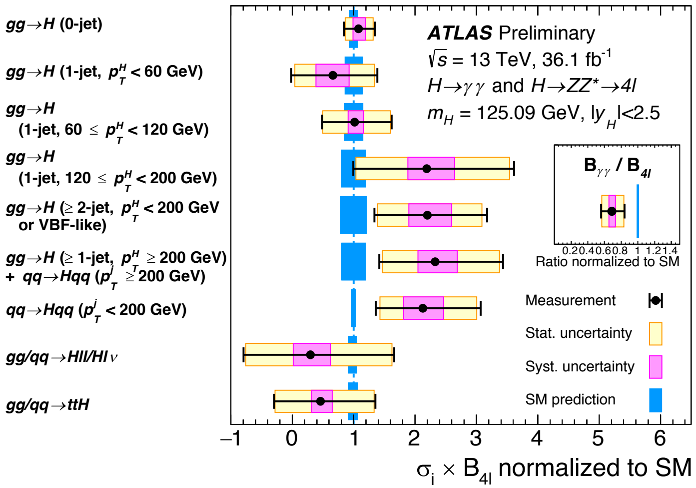

- The results show good overall agreement with the SM predictions in a range of kinematic regions of Higgs boson production processes
- The ten-dimensional compatibility between the measurement and the SM prediction corresponds to a p-value of $p_{SM} = 9\%$

Measurement region	Result	Uncertainty Total	Stat.	Syst.	SM prediction
$B_{\gamma\gamma}/B_{4\ell}$	12.5	${}^{+2.8}_{-2.3}$	$\left({}^{+2.6}_{-2.2}\right.$	$\left.{}^{+0.8}_{-0.6}\right)$	18.1 ± 0.2
$gg \to H$ (0-jet)	29.7	${}^{+7.3}_{-6.4}$	$\left({}^{+6.6}_{-6.0}\right.$	$\left.{}^{+3.1}_{-2.4}\right)$ pb	27.6 ± 1.9 pb
$gg \to H$ (1-jet, $p_T^H < 60$ GeV)	4.4	${}^{+4.8}_{-4.5}$	$\left({}^{+4.4}_{-4.1}\right.$	$\left.{}^{+1.7}_{-1.8}\right)$ pb	6.6 ± 0.9 pb
$gg \to H$ (1-jet, $60 \leq p_T^H < 120$ GeV)	4.6	${}^{+2.8}_{-2.4}$	$\left({}^{+2.7}_{-2.4}\right.$	$\left.{}^{+0.7}_{-0.5}\right)$ pb	4.6 ± 0.7 pb
$gg \to H$ (1-jet, $120 \leq p_T^H < 200$ GeV)	1.6	${}^{+1.1}_{-0.9}$	$\left({}^{+1.0}_{-0.9}\right.$	$\left.{}^{+0.3}_{-0.2}\right)$ pb	0.75 ± 0.15 pb
$gg \to H$ ($\geq$ 2-jet, $p_T^H < 200$ GeV or VBF-like)	10.6	${}^{+4.7}_{-4.2}$	$\left({}^{+4.3}_{-3.9}\right.$	$\left.{}^{+1.9}_{-1.4}\right)$ pb	4.8 ± 1.0 pb
$gg \to H$ ($\geq$ 1-jet, $p_T^H \geq 200$ GeV) + $qq \to Hqq$ ($p_T^j \geq 200$ GeV)	1.9	${}^{+0.9}_{-0.7}$	$\left({}^{+0.8}_{-0.7}\right.$	$\left.{}^{+0.3}_{-0.2}\right)$ pb	0.81 ± 0.16 pb
$qq \to Hqq$ ($p_T^j < 200$ GeV)	9.8	${}^{+4.3}_{-3.5}$	$\left({}^{+4.0}_{-3.2}\right.$	$\left.{}^{+1.5}_{-1.4}\right)$ pb	$4.58^{+0.15}_{-0.18}$ pb
$gg/qq \to H\ell\ell/H\ell\nu$	0.2	${}^{+0.9}_{-0.7}$	$\left({}^{+0.8}_{-0.7}\right.$	$\left.\pm 0.2\right)$ pb	$0.63^{+0.03}_{-0.06}$ pb
$q\bar{q}/gg \to t\bar{t}H$	0.3	${}^{+0.5}_{-0.4}$	$\left({}^{+0.5}_{-0.4}\right.$	$\left.\pm 0.1\right)$ pb	$0.59^{+0.04}_{-0.05}$ pb

κ framework

- The κ framework parameterizes new Higgs boson interactions as multiplicative coefficients to cross sections and partial widths
- $\sigma(i \to H \to f) = \kappa_i^2 \sigma_i^{SM} \frac{\kappa_f^2 \Gamma_f^{SM}}{\kappa_H^2 \Gamma_H^{SM}}$
- First, two-parameter fits are performed for the coefficients of couplings to fermions (κ_f) and to weak vector bosons (κ_V)

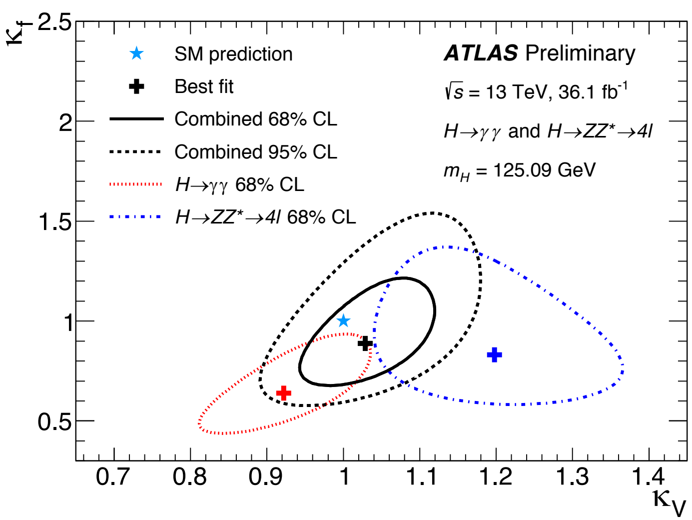

- A small positive correlation due in part to the destructive interference between the top-quark and W-boson loops in the $H \to \gamma\gamma$ decay
- The correlation between the two quantities is estimated to be 54%
- $\kappa_V = 1.03 \pm 0.06$
- $\kappa_f = 0.89^{+0.20}_{-0.15}$

> - Run1 result with all decay channels ($\gamma\gamma$,ZZ^*,$Z\gamma$,WW^*,$b\bar{b}$,$\tau\tau$,$\mu\mu$)
> - $\kappa_V = 1.09 \pm 0.07$
> - $\kappa_f = 1.11^{+0.16}_{-0.16}$

- Comparing to Run I results, κ_f errors are larger (40%) because Run I measurements contain more Yukawa couplings ($Z\gamma$, $b\bar{b}$, $\tau\tau$, $\mu\mu$)
- The two-dimensional compatibility with the SM prediction is $p_{SM} = 52\%$

κ_g, κ_γ

- The effective couplings κ_g and κ_γ capture all loop contributions to the Higgs-boson interaction with gluons and photons
- New loop processes would appear in these modifiers rather than being absorbed by the κ_f and κ_V modifiers

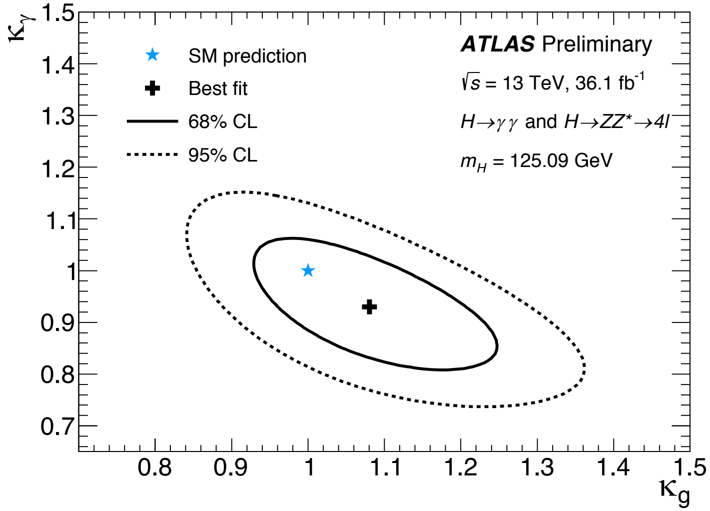

- Run1 result with all decay channels ($\gamma\gamma$,ZZ^*,$Z\gamma$,WW^*,$b\bar{b}$,$\tau\tau$,$\mu\mu$)
- $\kappa_g = 1.12^{+0.14}_{-0.11}$
- $\kappa_\gamma = 1.00^{+0.12}_{-0.12}$

- A strong anti-correlation because the leading constraint comes from $H \rightarrow \gamma\gamma$ in the gluon fusion channel
- The correlation between the two quantities is estimated to be -64%
- $\kappa_g = 1.08^{+0.11}_{-0.10}$
- $\kappa_\gamma = 0.93^{+0.09}_{-0.08}$

- Comparing to Run I results, errors decrease by 12%/19% (κ_g/κ_γ)
- The two-dimensional compatibility with the SM prediction is $p_{SM} = 68\%$

Generic model

- A set of four ratios is constructed to probe the loop vertices, total width, and the fermion and vector couplings
- $\kappa_{gV} = \kappa_g \kappa_V / \kappa_H$
- $\lambda_{Vg} = \kappa_V / \kappa_g$
- $\lambda_{fg} = \kappa_f / \kappa_g$
- $\lambda_{\gamma V} = \kappa_\gamma / \kappa_V$
- The inclusion of κ_H in the parameterization allows for non-SM decays of the Higgs boson

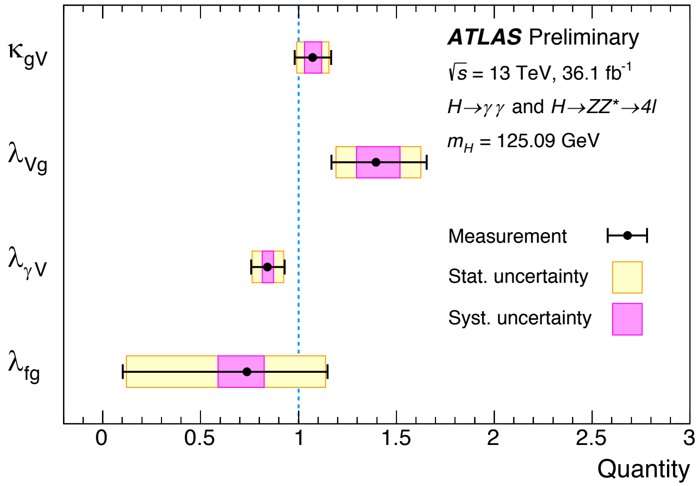

Parameter	Result	Uncertainty			
		Total	Stat.	Exp.	Th.
κ_{gV}	1.07	± 0.09	± 0.08	± 0.03	$^{+0.04}_{-0.03}$
λ_{Vg}	1.41	$^{+0.26}_{-0.23}$	$^{+0.23}_{-0.20}$	$^{+0.08}_{-0.06}$	$^{+0.09}_{-0.08}$
$\lambda_{\gamma V}$	0.84	$^{+0.09}_{-0.08}$	± 0.08	$^{+0.03}_{-0.02}$	± 0.01
λ_{fg}	0.74	$^{+0.41}_{-0.63}$	$^{+0.40}_{-0.62}$	$^{+0.06}_{-0.14}$	$^{+0.07}_{-0.05}$

- The four-dimensional compatibility with the SM prediction is $p_{SM} = 15\%$

Summary

- Higgs boson productions and decays combination measurements
  - The total cross section at $\sqrt{s} = 13\ TeV$ is measured to be $57.0^{+6.0}_{-5.9}(stat.)^{+4.0}_{-3.3}(syst.)\ pb$
  - The global signal strength is 1.09 ± 0.12
  - All results of production cross sections, ratio of cross sections, simplified template cross sections and κ frameworks were performed
  - No significant deviation from the Standard Model predictions is observed
  - The combination with more channels ($b\bar{b}$, $t\bar{t}H(ML)$) in Run II is ongoing!

Backup

ATLAS+CMS Run I Combination Results

$\sigma \cdot B$

Production process		$H \to \gamma\gamma$ [fb] Best fit value	Uncertainty Stat	Syst	$H \to ZZ$ [fb] Best fit value	Uncertainty Stat	Syst	$H \to WW$ [pb] Best fit value	Uncertainty Stat	Syst	$H \to \tau\tau$ [fb] Best fit value	Uncertainty Stat	Syst	$H \to bb$ [pb] Best fit value	Uncertainty Stat	Syst
ggF	Measured	$48.0^{+10.0}_{-9.7}$	$^{+9.4}_{-9.4}$	$^{+3.2}_{-2.3}$	580^{+170}_{-160}	$^{+170}_{-160}$	$^{+40}_{-40}$	$3.5^{+0.7}_{-0.7}$	$^{+0.5}_{-0.5}$	$^{+0.5}_{-0.5}$	1300^{+700}_{-700}	$^{+400}_{-400}$	$^{+500}_{-500}$	–		
		$\left(^{+9.7}_{-9.5}\right)$	$\left(^{+9.4}_{-9.4}\right)$	$\left(^{+2.5}_{-1.6}\right)$	$\left(^{+150}_{-130}\right)$	$\left(^{+140}_{-130}\right)$	$\left(^{+30}_{-20}\right)$	$\left(^{+0.7}_{-0.7}\right)$	$\left(^{+0.5}_{-0.5}\right)$	$\left(^{+0.5}_{-0.5}\right)$	$\left(^{+700}_{-700}\right)$	$\left(^{+400}_{-400}\right)$	$\left(^{+500}_{-500}\right)$	–		
	Predicted	44 ± 5			510 ± 60			4.1 ± 0.5			1210 ± 140			11.0 ± 1.2		
	Ratio	$1.10^{+0.23}_{-0.22}$	$^{+0.22}_{-0.21}$	$^{+0.07}_{-0.05}$	$1.13^{+0.34}_{-0.31}$	$^{+0.33}_{-0.30}$	$^{+0.09}_{-0.07}$	$0.84^{+0.17}_{-0.17}$	$^{+0.12}_{-0.12}$	$^{+0.12}_{-0.11}$	$1.0^{+0.6}_{-0.6}$	$^{+0.4}_{-0.4}$	$^{+0.4}_{-0.4}$	–		
VBF	Measured	$4.6^{+1.9}_{-1.8}$	$^{+1.8}_{-1.7}$	$^{+0.6}_{-0.5}$	3^{+46}_{-26}	$^{+46}_{-25}$	$^{+7}_{-7}$	$0.39^{+0.14}_{-0.13}$	$^{+0.13}_{-0.12}$	$^{+0.07}_{-0.05}$	125^{+39}_{-37}	$^{+34}_{-32}$	$^{+19}_{-18}$	–		
		$\left(^{+1.8}_{-1.6}\right)$	$\left(^{+1.7}_{-1.6}\right)$	$\left(^{+0.5}_{-0.4}\right)$	$\left(^{+60}_{-39}\right)$	$\left(^{+60}_{-39}\right)$	$\left(^{+8}_{-5}\right)$	$\left(^{+0.15}_{-0.13}\right)$	$\left(^{+0.13}_{-0.12}\right)$	$\left(^{+0.07}_{-0.06}\right)$	$\left(^{+39}_{-37}\right)$	$\left(^{+34}_{-32}\right)$	$\left(^{+19}_{-18}\right)$	–		
	Predicted	3.60 ± 0.20			42.2 ± 2.0			0.341 ± 0.017			100 ± 6			0.91 ± 0.04		
	Ratio	$1.3^{+0.5}_{-0.5}$	$^{+0.5}_{-0.5}$	$^{+0.2}_{-0.1}$	$0.1^{+1.1}_{-0.6}$	$^{+1.1}_{-0.6}$	$^{+0.2}_{-0.2}$	$1.2^{+0.4}_{-0.4}$	$^{+0.4}_{-0.3}$	$^{+0.2}_{-0.2}$	$1.3^{+0.4}_{-0.4}$	$^{+0.3}_{-0.3}$	$^{+0.2}_{-0.2}$	–		
WH	Measured	$0.7^{+2.1}_{-1.9}$	$^{+2.1}_{-1.8}$	$^{+0.3}_{-0.3}$	–			$0.24^{+0.18}_{-0.16}$	$^{+0.15}_{-0.14}$	$^{+0.10}_{-0.08}$	-64^{+64}_{-61}	$^{+55}_{-50}$	$^{+32}_{-34}$	$0.42^{+0.21}_{-0.20}$	$^{+0.17}_{-0.16}$	$^{+0.12}_{-0.11}$
		$\left(^{+1.9}_{-1.8}\right)$	$\left(^{+1.9}_{-1.8}\right)$	$\left(^{+0.1}_{-0.1}\right)$	–			$\left(^{+0.16}_{-0.14}\right)$	$\left(^{+0.14}_{-0.13}\right)$	$\left(^{+0.08}_{-0.07}\right)$	$\left(^{+67}_{-64}\right)$	$\left(^{+60}_{-54}\right)$	$\left(^{+30}_{-32}\right)$	$\left(^{+0.22}_{-0.21}\right)$	$\left(^{+0.18}_{-0.17}\right)$	$\left(^{+0.12}_{-0.11}\right)$
	Predicted	1.60 ± 0.09			18.8 ± 0.9			0.152 ± 0.007			44.3 ± 2.8			0.404 ± 0.017		
	Ratio	$0.5^{+1.3}_{-1.2}$	$^{+1.3}_{-1.1}$	$^{+0.2}_{-0.2}$	–			$1.6^{+1.2}_{-1.0}$	$^{+1.0}_{-0.9}$	$^{+0.6}_{-0.5}$	$-1.4^{+1.4}_{-1.4}$	$^{+1.2}_{-1.1}$	$^{+0.7}_{-0.8}$	$1.0^{+0.5}_{-0.5}$	$^{+0.4}_{-0.4}$	$^{+0.3}_{-0.3}$
ZH	Measured	$0.5^{+2.9}_{-2.4}$	$^{+2.8}_{-2.3}$	$^{+0.5}_{-0.2}$	–			$0.53^{+0.23}_{-0.20}$	$^{+0.21}_{-0.19}$	$^{+0.10}_{-0.07}$	58^{+56}_{-47}	$^{+52}_{-44}$	$^{+20}_{-16}$	$0.08^{+0.09}_{-0.09}$	$^{+0.08}_{-0.08}$	$^{+0.04}_{-0.04}$
		$\left(^{+2.3}_{-1.9}\right)$	$\left(^{+2.3}_{-1.9}\right)$	$\left(^{+0.1}_{-0.1}\right)$	–			$\left(^{+0.17}_{-0.14}\right)$	$\left(^{+0.16}_{-0.14}\right)$	$\left(^{+0.05}_{-0.04}\right)$	$\left(^{+49}_{-40}\right)$	$\left(^{+46}_{-38}\right)$	$\left(^{+16}_{-12}\right)$	$\left(^{+0.10}_{-0.09}\right)$	$\left(^{+0.09}_{-0.08}\right)$	$\left(^{+0.05}_{-0.04}\right)$
	Predicted	0.94 ± 0.06			11.1 ± 0.6			0.089 ± 0.005			26.1 ± 1.8			0.238 ± 0.012		
	Ratio	$0.5^{+3.0}_{-2.5}$	$^{+3.0}_{-2.5}$	$^{+0.5}_{-0.2}$	–			$5.9^{+2.6}_{-2.2}$	$^{+2.3}_{-2.1}$	$^{+1.1}_{-0.8}$	$2.2^{+2.2}_{-1.8}$	$^{+2.0}_{-1.7}$	$^{+0.8}_{-0.6}$	$0.4^{+0.4}_{-0.4}$	$^{+0.3}_{-0.3}$	$^{+0.2}_{-0.2}$
ttH	Measured	$0.64^{+0.48}_{-0.38}$	$^{+0.48}_{-0.38}$	$^{+0.07}_{-0.04}$	–			$0.14^{+0.05}_{-0.05}$	$^{+0.04}_{-0.04}$	$^{+0.03}_{-0.03}$	-15^{+30}_{-26}	$^{+26}_{-22}$	$^{+15}_{-15}$	$0.08^{+0.07}_{-0.07}$	$^{+0.04}_{-0.04}$	$^{+0.06}_{-0.06}$
		$\left(^{+0.45}_{-0.34}\right)$	$\left(^{+0.44}_{-0.33}\right)$	$\left(^{+0.10}_{-0.05}\right)$	–			$\left(^{+0.04}_{-0.04}\right)$	$\left(^{+0.04}_{-0.04}\right)$	$\left(^{+0.02}_{-0.02}\right)$	$\left(^{+31}_{-26}\right)$	$\left(^{+26}_{-22}\right)$	$\left(^{+16}_{-13}\right)$	$\left(^{+0.07}_{-0.06}\right)$	$\left(^{+0.04}_{-0.04}\right)$	$\left(^{+0.06}_{-0.05}\right)$
	Predicted	0.294 ± 0.035			3.4 ± 0.4			0.0279 ± 0.0032			8.1 ± 1.0			0.074 ± 0.008		
	Ratio	$2.2^{+1.6}_{-1.3}$	$^{+1.6}_{-1.3}$	$^{+0.2}_{-0.1}$	–			$5.0^{+1.8}_{-1.7}$	$^{+1.5}_{-1.5}$	$^{+1.0}_{-0.9}$	$-1.9^{+3.7}_{-3.3}$	$^{+3.2}_{-2.7}$	$^{+1.9}_{-1.8}$	$1.1^{+1.0}_{-1.0}$	$^{+0.5}_{-0.5}$	$^{+0.8}_{-0.8}$

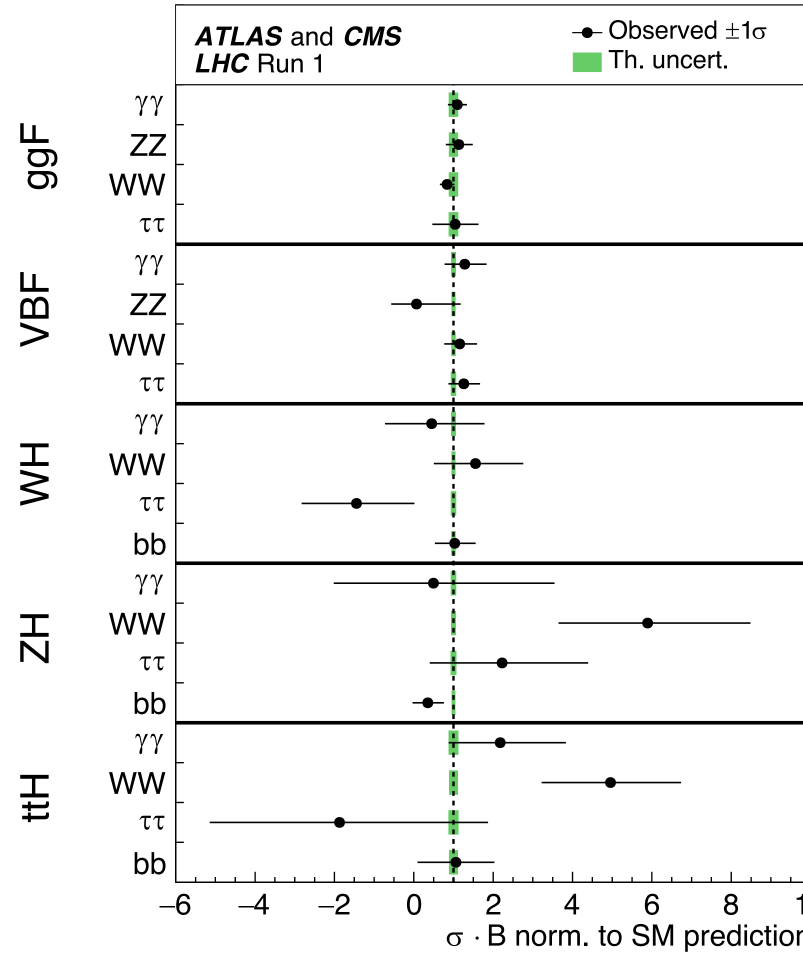

Ratio of cross sections and branching ratios

Production process		Decay mode														
		$H \to \gamma\gamma$ [fb]			$H \to ZZ$ [fb]			$H \to WW$ [pb]			$H \to \tau\tau$ [fb]			$H \to bb$ [pb]		
		Best fit value	Uncertainty Stat	Syst	Best fit value	Uncertainty Stat	Syst	Best fit value	Uncertainty Stat	Syst	Best fit value	Uncertainty Stat	Syst	Best fit value	Uncertainty Stat	Syst
ggF	Measured	$48.0^{+10.0}_{-9.7}$	$^{+9.4}_{-9.4}$	$^{+3.2}_{-2.3}$	580^{+170}_{-160}	$^{+170}_{-160}$	$^{+40}_{-40}$	$3.5^{+0.7}_{-0.7}$	$^{+0.5}_{-0.5}$	$^{+0.5}_{-0.5}$	1300^{+700}_{-700}	$^{+400}_{-400}$	$^{+500}_{-500}$	–		
		$\left(^{+9.7}_{-9.5}\right)$	$\left(^{+9.4}_{-9.4}\right)$	$\left(^{+2.5}_{-1.6}\right)$	$\left(^{+150}_{-130}\right)$	$\left(^{+140}_{-130}\right)$	$\left(^{+30}_{-20}\right)$	$\left(^{+0.7}_{-0.7}\right)$	$\left(^{+0.5}_{-0.5}\right)$	$\left(^{+0.5}_{-0.5}\right)$	$\left(^{+700}_{-700}\right)$	$\left(^{+400}_{-400}\right)$	$\left(^{+500}_{-500}\right)$	–		
	Predicted	44 ± 5			510 ± 60			4.1 ± 0.5			1210 ± 140			11.0 ± 1.2		
	Ratio	$1.10^{+0.23}_{-0.22}$	$^{+0.22}_{-0.21}$	$^{+0.07}_{-0.05}$	$1.13^{+0.34}_{-0.31}$	$^{+0.33}_{-0.30}$	$^{+0.09}_{-0.07}$	$0.84^{+0.17}_{-0.17}$	$^{+0.12}_{-0.12}$	$^{+0.12}_{-0.11}$	$1.0^{+0.6}_{-0.6}$	$^{+0.4}_{-0.4}$	$^{+0.4}_{-0.4}$	–		
VBF	Measured	$4.6^{+1.9}_{-1.8}$	$^{+1.8}_{-1.7}$	$^{+0.6}_{-0.5}$	3^{+46}_{-26}	$^{+46}_{-25}$	$^{+7}_{-7}$	$0.39^{+0.14}_{-0.13}$	$^{+0.13}_{-0.12}$	$^{+0.07}_{-0.05}$	125^{+39}_{-37}	$^{+34}_{-32}$	$^{+19}_{-18}$	–		
		$\left(^{+1.8}_{-1.6}\right)$	$\left(^{+1.7}_{-1.6}\right)$	$\left(^{+0.5}_{-0.4}\right)$	$\left(^{+60}_{-39}\right)$	$\left(^{+60}_{-39}\right)$	$\left(^{+8}_{-5}\right)$	$\left(^{+0.15}_{-0.13}\right)$	$\left(^{+0.13}_{-0.12}\right)$	$\left(^{+0.07}_{-0.06}\right)$	$\left(^{+39}_{-37}\right)$	$\left(^{+34}_{-32}\right)$	$\left(^{+19}_{-18}\right)$	–		
	Predicted	3.60 ± 0.20			42.2 ± 2.0			0.341 ± 0.017			100 ± 6			0.91 ± 0.04		
	Ratio	$1.3^{+0.5}_{-0.5}$	$^{+0.5}_{-0.5}$	$^{+0.2}_{-0.1}$	$0.1^{+1.1}_{-0.6}$	$^{+1.1}_{-0.6}$	$^{+0.2}_{-0.2}$	$1.2^{+0.4}_{-0.4}$	$^{+0.4}_{-0.3}$	$^{+0.2}_{-0.2}$	$1.3^{+0.4}_{-0.4}$	$^{+0.3}_{-0.3}$	$^{+0.2}_{-0.2}$	–		
WH	Measured	$0.7^{+2.1}_{-1.9}$	$^{+2.1}_{-1.8}$	$^{+0.3}_{-0.3}$	–			$0.24^{+0.18}_{-0.16}$	$^{+0.15}_{-0.14}$	$^{+0.10}_{-0.08}$	-64^{+64}_{-61}	$^{+55}_{-50}$	$^{+32}_{-34}$	$0.42^{+0.21}_{-0.20}$	$^{+0.17}_{-0.16}$	$^{+0.12}_{-0.11}$
		$\left(^{+1.9}_{-1.8}\right)$	$\left(^{+1.9}_{-1.8}\right)$	$\left(^{+0.1}_{-0.1}\right)$	–			$\left(^{+0.16}_{-0.14}\right)$	$\left(^{+0.14}_{-0.13}\right)$	$\left(^{+0.08}_{-0.07}\right)$	$\left(^{+67}_{-64}\right)$	$\left(^{+60}_{-54}\right)$	$\left(^{+30}_{-32}\right)$	$\left(^{+0.22}_{-0.21}\right)$	$\left(^{+0.18}_{-0.17}\right)$	$\left(^{+0.12}_{-0.11}\right)$
	Predicted	1.60 ± 0.09			18.8 ± 0.9			0.152 ± 0.007			44.3 ± 2.8			0.404 ± 0.017		
	Ratio	$0.5^{+1.3}_{-1.2}$	$^{+1.3}_{-1.1}$	$^{+0.2}_{-0.2}$	–			$1.6^{+1.2}_{-1.0}$	$^{+1.0}_{-0.9}$	$^{+0.6}_{-0.5}$	$-1.4^{+1.4}_{-1.4}$	$^{+1.2}_{-1.1}$	$^{+0.7}_{-0.8}$	$1.0^{+0.5}_{-0.5}$	$^{+0.4}_{-0.4}$	$^{+0.3}_{-0.3}$
ZH	Measured	$0.5^{+2.9}_{-2.4}$	$^{+2.8}_{-2.3}$	$^{+0.5}_{-0.2}$	–			$0.53^{+0.23}_{-0.20}$	$^{+0.21}_{-0.19}$	$^{+0.10}_{-0.07}$	58^{+56}_{-47}	$^{+52}_{-44}$	$^{+20}_{-16}$	$0.08^{+0.09}_{-0.09}$	$^{+0.08}_{-0.08}$	$^{+0.04}_{-0.04}$
		$\left(^{+2.3}_{-1.9}\right)$	$\left(^{+2.3}_{-1.9}\right)$	$\left(^{+0.1}_{-0.1}\right)$	–			$\left(^{+0.17}_{-0.14}\right)$	$\left(^{+0.16}_{-0.14}\right)$	$\left(^{+0.05}_{-0.04}\right)$	$\left(^{+49}_{-40}\right)$	$\left(^{+46}_{-38}\right)$	$\left(^{+16}_{-12}\right)$	$\left(^{+0.10}_{-0.09}\right)$	$\left(^{+0.09}_{-0.08}\right)$	$\left(^{+0.05}_{-0.04}\right)$
	Predicted	0.94 ± 0.06			11.1 ± 0.6			0.089 ± 0.005			26.1 ± 1.8			0.238 ± 0.012		
	Ratio	$0.5^{+3.0}_{-2.5}$	$^{+3.0}_{-2.5}$	$^{+0.5}_{-0.2}$	–			$5.9^{+2.6}_{-2.2}$	$^{+2.3}_{-2.1}$	$^{+1.1}_{-0.8}$	$2.2^{+2.2}_{-1.8}$	$^{+2.0}_{-1.7}$	$^{+0.8}_{-0.6}$	$0.4^{+0.4}_{-0.4}$	$^{+0.3}_{-0.3}$	$^{+0.2}_{-0.2}$
ttH	Measured	$0.64^{+0.48}_{-0.38}$	$^{+0.48}_{-0.38}$	$^{+0.07}_{-0.04}$	–			$0.14^{+0.05}_{-0.05}$	$^{+0.04}_{-0.04}$	$^{+0.03}_{-0.03}$	-15^{+30}_{-26}	$^{+26}_{-22}$	$^{+15}_{-15}$	$0.08^{+0.07}_{-0.07}$	$^{+0.04}_{-0.04}$	$^{+0.06}_{-0.06}$
		$\left(^{+0.45}_{-0.34}\right)$	$\left(^{+0.44}_{-0.33}\right)$	$\left(^{+0.10}_{-0.05}\right)$	–			$\left(^{+0.04}_{-0.04}\right)$	$\left(^{+0.04}_{-0.04}\right)$	$\left(^{+0.02}_{-0.02}\right)$	$\left(^{+31}_{-26}\right)$	$\left(^{+26}_{-22}\right)$	$\left(^{+16}_{-13}\right)$	$\left(^{+0.07}_{-0.06}\right)$	$\left(^{+0.04}_{-0.04}\right)$	$\left(^{+0.06}_{-0.05}\right)$
	Predicted	0.294 ± 0.035			3.4 ± 0.4			0.0279 ± 0.0032			8.1 ± 1.0			0.074 ± 0.008		
	Ratio	$2.2^{+1.6}_{-1.3}$	$^{+1.6}_{-1.3}$	$^{+0.2}_{-0.1}$	–			$5.0^{+1.8}_{-1.7}$	$^{+1.5}_{-1.5}$	$^{+1.0}_{-0.9}$	$-1.9^{+3.7}_{-3.3}$	$^{+3.2}_{-2.7}$	$^{+1.9}_{-1.8}$	$1.1^{+1.0}_{-1.0}$	$^{+0.5}_{-0.5}$	$^{+0.8}_{-0.8}$

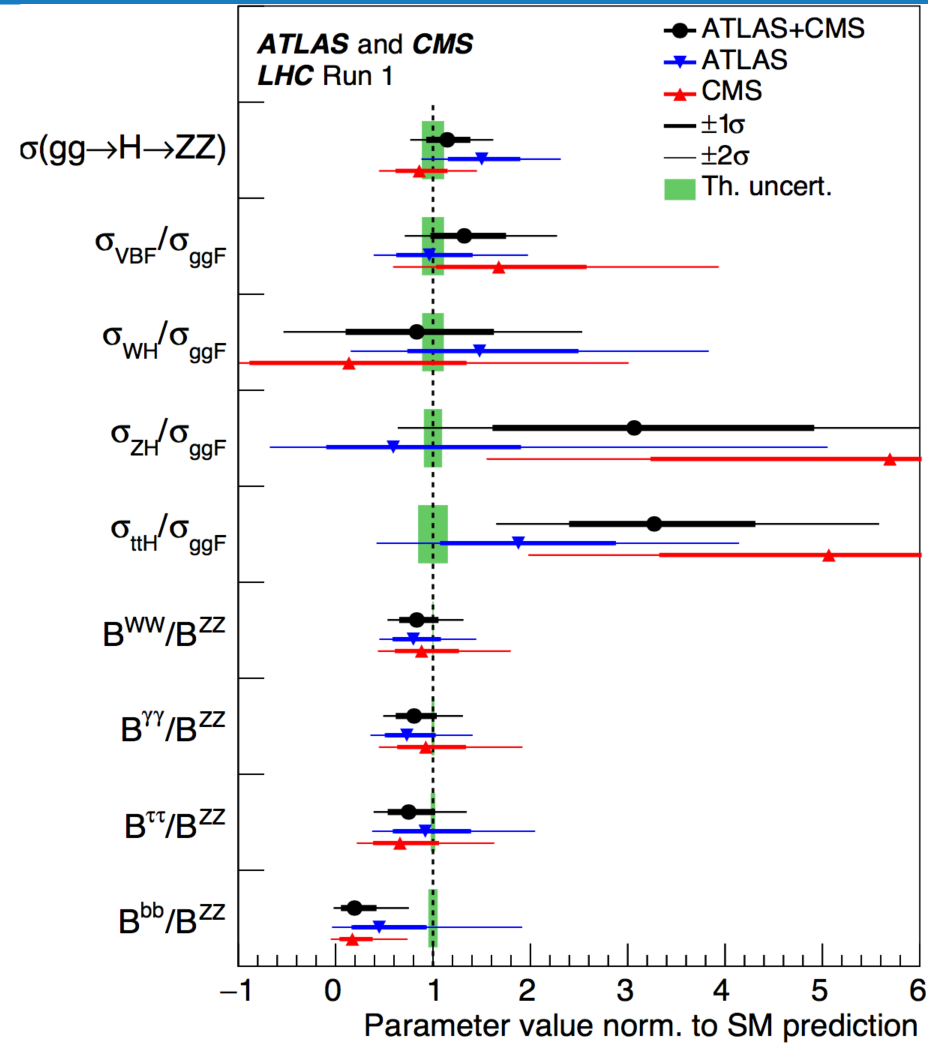

- The p-value of the compatibility between the data and the SM predictions is 16%
- Most measurements are consistent with the SM predictions within less than 2σ

Global signal strength

- $\mu = 1.09^{+0.11}_{-0.10}\left(\pm 0.07(stat.) \pm 0.04(exp.) \pm 0.03(thBkg.)^{+0.07}_{-0.06}(thSig)\right)$
- This result is consistent with the SM prediction of $\mu = 1$ within less than 1σ
- The *p*-value of the compatibility between the data and the SM predictions is 40%

	Best fit μ	Uncertainty				
		Total	Stat	Expt	Thbgd	Thsig
ATLAS + CMS (measured)	1.09	$^{+0.11}_{-0.10}$	$^{+0.07}_{-0.07}$	$^{+0.04}_{-0.04}$	$^{+0.03}_{-0.03}$	$^{+0.07}_{-0.06}$
ATLAS + CMS (expected)		$^{+0.11}_{-0.10}$	$^{+0.07}_{-0.07}$	$^{+0.04}_{-0.04}$	$^{+0.03}_{-0.03}$	$^{+0.07}_{-0.06}$
ATLAS (measured)	1.20	$^{+0.15}_{-0.14}$	$^{+0.10}_{-0.10}$	$^{+0.06}_{-0.06}$	$^{+0.04}_{-0.04}$	$^{+0.08}_{-0.07}$
ATLAS (expected)		$^{+0.14}_{-0.13}$	$^{+0.10}_{-0.10}$	$^{+0.06}_{-0.05}$	$^{+0.04}_{-0.04}$	$^{+0.07}_{-0.06}$
CMS (measured)	0.97	$^{+0.14}_{-0.13}$	$^{+0.09}_{-0.09}$	$^{+0.05}_{-0.05}$	$^{+0.04}_{-0.03}$	$^{+0.07}_{-0.06}$
CMS (expected)		$^{+0.14}_{-0.13}$	$^{+0.09}_{-0.09}$	$^{+0.05}_{-0.05}$	$^{+0.04}_{-0.03}$	$^{+0.08}_{-0.06}$

Signal strengths of production processes

Production process	ATLAS+CMS	ATLAS	CMS
μ_{ggF}	$1.03\,^{+0.16}_{-0.14}$ $\left(^{+0.16}_{-0.14}\right)$	$1.26\,^{+0.23}_{-0.20}$ $\left(^{+0.21}_{-0.18}\right)$	$0.84\,^{+0.18}_{-0.16}$ $\left(^{+0.20}_{-0.17}\right)$
μ_{VBF}	$1.18\,^{+0.25}_{-0.23}$ $\left(^{+0.24}_{-0.23}\right)$	$1.21\,^{+0.33}_{-0.30}$ $\left(^{+0.32}_{-0.29}\right)$	$1.14\,^{+0.37}_{-0.34}$ $\left(^{+0.36}_{-0.34}\right)$
μ_{WH}	$0.89\,^{+0.40}_{-0.38}$ $\left(^{+0.41}_{-0.39}\right)$	$1.25\,^{+0.56}_{-0.52}$ $\left(^{+0.56}_{-0.53}\right)$	$0.46\,^{+0.57}_{-0.53}$ $\left(^{+0.60}_{-0.57}\right)$
μ_{ZH}	$0.79\,^{+0.38}_{-0.36}$ $\left(^{+0.39}_{-0.36}\right)$	$0.30\,^{+0.51}_{-0.45}$ $\left(^{+0.55}_{-0.51}\right)$	$1.35\,^{+0.58}_{-0.54}$ $\left(^{+0.55}_{-0.51}\right)$
μ_{ttH}	$2.3\,^{+0.7}_{-0.6}$ $\left(^{+0.5}_{-0.5}\right)$	$1.9\,^{+0.8}_{-0.7}$ $\left(^{+0.7}_{-0.7}\right)$	$2.9\,^{+1.0}_{-0.9}$ $\left(^{+0.9}_{-0.8}\right)$

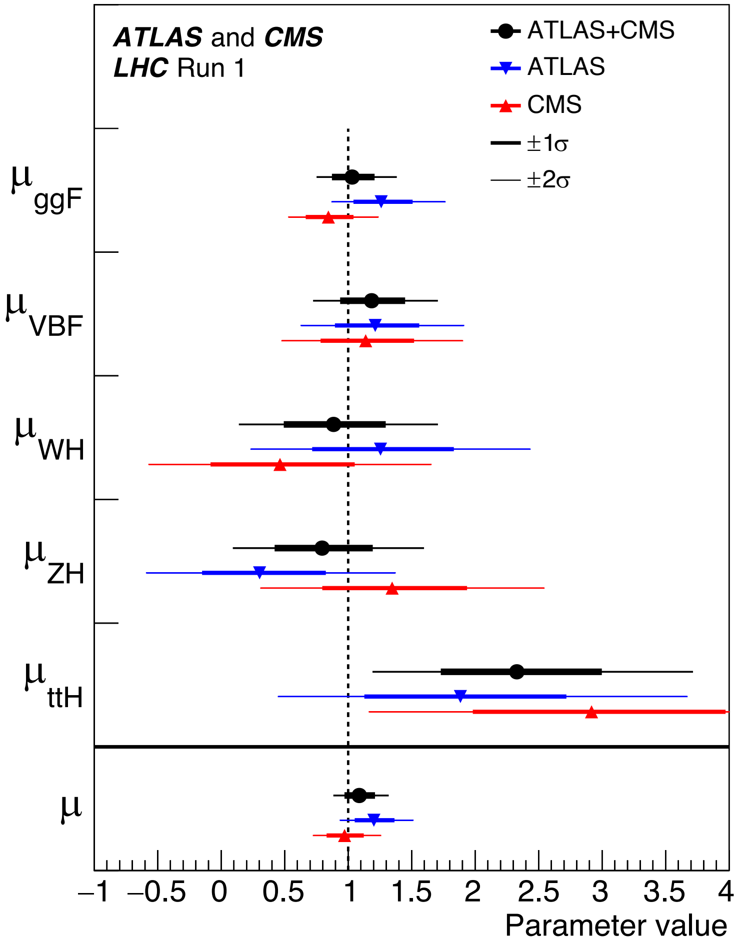

- The *p*-value of the compatibility between the data and the SM predictions is 24%

Signal strengths of decay channels

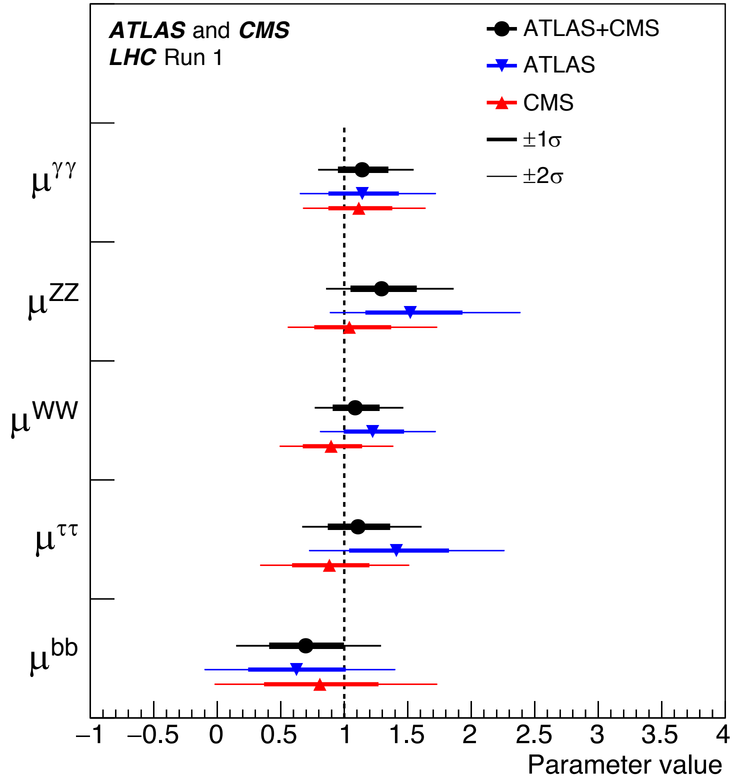

Decay channel	ATLAS+CMS	ATLAS	CMS
$\mu^{\gamma\gamma}$	$1.14\ ^{+0.19}_{-0.18}$ $\left(^{+0.18}_{-0.17}\right)$	$1.14\ ^{+0.27}_{-0.25}$ $\left(^{+0.26}_{-0.24}\right)$	$1.11\ ^{+0.25}_{-0.23}$ $\left(^{+0.23}_{-0.21}\right)$
μ^{ZZ}	$1.29\ ^{+0.26}_{-0.23}$ $\left(^{+0.23}_{-0.20}\right)$	$1.52\ ^{+0.40}_{-0.34}$ $\left(^{+0.32}_{-0.27}\right)$	$1.04\ ^{+0.32}_{-0.26}$ $\left(^{+0.30}_{-0.25}\right)$
μ^{WW}	$1.09\ ^{+0.18}_{-0.16}$ $\left(^{+0.16}_{-0.15}\right)$	$1.22\ ^{+0.23}_{-0.21}$ $\left(^{+0.21}_{-0.20}\right)$	$0.90\ ^{+0.23}_{-0.21}$ $\left(^{+0.23}_{-0.20}\right)$
$\mu^{\tau\tau}$	$1.11\ ^{+0.24}_{-0.22}$ $\left(^{+0.24}_{-0.22}\right)$	$1.41\ ^{+0.40}_{-0.36}$ $\left(^{+0.37}_{-0.33}\right)$	$0.88\ ^{+0.30}_{-0.28}$ $\left(^{+0.31}_{-0.29}\right)$
μ^{bb}	$0.70\ ^{+0.29}_{-0.27}$ $\left(^{+0.29}_{-0.28}\right)$	$0.62\ ^{+0.37}_{-0.37}$ $\left(^{+0.39}_{-0.37}\right)$	$0.81\ ^{+0.45}_{-0.43}$ $\left(^{+0.45}_{-0.43}\right)$
$\mu^{\mu\mu}$	$0.1\ ^{+2.5}_{-2.5}$ $\left(^{+2.4}_{-2.3}\right)$	$-0.6\ ^{+3.6}_{-3.6}$ $\left(^{+3.6}_{-3.6}\right)$	$0.9\ ^{+3.6}_{-3.5}$ $\left(^{+3.3}_{-3.2}\right)$

- The *p*-value of the compatibility between the data and the SM predictions is 75%

ATLAS+CMS Run I significance

Production process	Measured significance (σ)	Expected significance (σ)
VBF	5.4	4.6
WH	2.4	2.7
ZH	2.3	2.9
VH	3.5	4.2
ttH	4.4	2.0
Decay channel		
$H \to \tau\tau$	5.5	5.0
$H \to bb$	2.6	3.7

κ Framework

Modifier interpretation

- κ_g^2

13 TeV															
M_h [GeV]	σ_{EW} [pb]	σ_{tt} [pb]	σ_{tb} [pb]	σ_{bb} [pb]	σ_{tc} [pb]	σ_{bc} [pb]	σ_{cc} [pb]	σ_{tot} [pb]	σ_{QCD} [pb]	κ_t^2	$\kappa_t\kappa_b$	κ_b^2	$\kappa_t\kappa_c$	$\kappa_b\kappa_c$	κ_c^2
124.50	2.40	48.35	-1.76	0.10	-0.22	0.02	0.0009	48.89	46.49	1.040	-0.038	0.002	-0.005	0.0004	0.00002
125.00	2.39	48.00	-1.74	0.10	-0.22	0.02	0.0009	48.55	46.16	1.040	-0.038	0.002	-0.005	0.0004	0.00002
125.09	2.39	47.94	-1.73	0.10	-0.22	0.02	0.0009	48.50	46.11	1.040	-0.038	0.002	-0.005	0.0004	0.00002
125.50	2.39	47.65	-1.72	0.10	-0.22	0.02	0.0009	48.22	45.83	1.040	-0.038	0.002	-0.005	0.0004	0.00002

- κ_{VBF}^2

	7 TeV				8 TeV				13 TeV			
M_h [GeV]	σ_{WW} [pb]	σ_{ZZ} [pb]	κ_W^2	κ_Z^2	σ_{WW} [pb]	σ_{ZZ} [pb]	κ_W^2	κ_Z^2	σ_{WW}	σ_{ZZ}	κ_W^2	κ_Z^2
120.0	0.993	0.349	0.740	0.260	1.278	0.452	0.739	0.261	3.001	1.091	0.733	0.267
125.0	0.946	0.333	0.740	0.260	1.220	0.432	0.738	0.262	2.882	1.049	0.733	0.267

- κ_{tH}^2

13 TeV							
M_h [GeV]	σ_t^2 [fb]	σ_W^2 [fb]	$\sigma_t\sigma_W$ [fb]	σ(t-ch) [fb]	κ_t^2	κ_W^2	$\kappa_t\kappa_W$
125.00	195.5	265.7	-387.0	74.25	2.633	3.578	-5.211

- κ_{WH}^2

13 TeV							
M_h [GeV]	σ_t^2 [fb]	σ_W^2 [fb]	$\sigma_t\sigma_W$ [fb]	σ(tHW) [fb]	κ_t^2	κ_W^2	$\kappa_t\kappa_W$
125.00	44.13	35.05	-64.01	15.17	2.909	2.310	-4.220